Electrostatic influences of charged inner pore residues on the conductance and gating of small conductance Ca^{2+} activated K^+ channels

Weiyan Li and Richard W. Aldrich[1]

Section of Neurobiology, Center for Learning and Memory, University of Texas at Austin, Austin, TX 78712

This contribution is part of the special series of Inaugural Articles by members of the National Academy of Sciences elected in 2008.

Contributed by Richard W. Aldrich, February 23, 2011 (sent for review February 10, 2011)

SK channels underlie important physiological functions by linking calcium signaling with neuronal excitability. Potassium currents through SK channels demonstrate inward rectification, which further reduces their small outward conductance. Although it has been generally attributed to block of outward current by intracellular divalent ions, we find that inward rectification is in fact an intrinsic property of SK channels independent of intracellular blockers. We identified three charged residues in the S6 transmembrane domain of SK channels near the inner mouth of the pore that collectively control the conductance and rectification through an electrostatic mechanism. Additionally, electrostatic contributions from these residues also play an important role in determining the intrinsic open probability of SK channels in the absence of Ca^{2+}, affecting the apparent Ca^{2+} affinity for activation.

KCa 2.2 | KCNN2

Small conductance Ca^{2+} activated K^+ (SK, KCNN2, KCa2) channels are broadly expressed in excitable tissues, underlying a variety of physiological functions such as synaptic plasticity, regulation of blood pressure, and neuronal firing. Activation of SK channels by elevation of intracellular Ca^{2+} leads to efflux of K^+ ions, providing an essential link between Ca^{2+} signaling and neuronal excitability (1, 2). Ca^{2+} activates SK channels by binding to calmodulin molecules that are constitutively associated with channel subunits (3). Much of the interest in biophysical studies of SK channels has surrounded the mechanism for the coupling between calmodulin and the SK channel pore during gating, and significant progress has been made (4). By comparison, the mechanisms for the ion conduction and intrinsic energetics of the SK channel pore have been less studied. With symmetrical K^+ concentrations, K^+ current carried by SK channels demonstrates a significant inward rectification. SK channels have smaller single-channel conductance than other Ca^{2+} activated K^+ channels, and this rectification further reduces the amplitude of outward current. Earlier studies demonstrated that the voltage-dependent block of SK current by intracellular divalent ions can result in apparent inward rectification (5), leading to a conclusion generally accepted that all rectification is due to a divalent block of outward current (2). However, a careful look at the earlier findings indicates that other mechanisms must exist underlying the rectification of SK current. For example, the measured apparent affinities for divalent ions are too low to explain the observed level of rectification. Additionally, significant rectification still exists for SK channels carrying a mutation that dramatically reduces the affinities for divalent ions (6). In this study, we have identified an intrinsic mechanism for the inward rectification of SK channels that is independent of divalent block. Three charged residues near the inner mouth of the pore collectively influence the single-channel conductance and determines the level of rectification for SK channels, likely by an electrostatic effect on the entry rate of K^+ ions into the pore. Importantly, these charged residues also affect the apparent Ca^{2+} affinity for SK channel gating, and the open probability (P_o) of the channel in the absence of Ca^{2+}. Our results indicate that charged residues near the inner mouth of SK channels exert important electrostatic influences on the conductance and rectification, as well as on the intrinsic energetics of the gating transition.

Results

Inward Rectification Is an Intrinsic Property of SK Channels. SK current demonstrates significant inward rectification with equal K^+ concentrations on both sides of the membrane, such that the amplitude of current at +80 mV is only about half of that at −80 mV (Fig. 1*A*). It has been generally accepted that the rectification of SK channels is due to the voltage-dependent block of outward current by intracellular divalent ions (2). In order to separate the intrinsic inward rectification from the block by divalent ions, which are normally required for channel activation, we tried to activate SK channels with solutions containing much lower concentrations of divalent ions. In a previous study, we showed that nanomolar concentrations of terbium ions (Tb^{3+}) can fully activate SK channels (7). In Fig. 1*A*, the SK current activated by 10 nM Tb^{3+} added to Chelex-100 column-treated bath solution (contaminating Ca^{2+} = ~200 nM) demonstrates a similar amount of inward rectification as that activated by 7.7 μM Ca^{2+}. It is unlikely that 10 nM Tb^{3+} blocks outward SK current, because much higher concentrations of Tb^{3+} (up to 80 nM) did not result in further reduction in outward current (7). SK channels can also be fully activated by lower concentrations of Ca^{2+} in the presence of enhancers such as NS309 (3-oxime-6,7-dichloro-1H-indole-2,3-dione) (8, 9). In Fig. 1*A*, SK current activated by 200 nM Ca^{2+} in the presence of 100 μM NS309 also demonstrates a similar amount of rectification. The fact that in both cases SK currents in the presence of approximately 200 nM Ca^{2+} demonstrate virtually the same level of inward rectification as those in 7.7 μM Ca^{2+} indicates that the observed inward rectification in Fig. 1*A* is not due to block by Ca^{2+}. It is formally possible that block by contaminating divalent ions other than Ca^{2+} may have resulted in this rectification. However, given the presence of different Ca^{2+} chelators or Chelex-100 treatment, it seems unlikely that in the three different solutions the concentrations of the contaminating divalent ions would happen to be the same. Instead, these data strongly suggest that the rectification seen in Fig. 1*A* is an intrinsic property of SK channels independent of divalent block.

Charged Residues Near the Inner Mouth Control Inward Rectification by Regulating Outward Single-Channel Conductance. In order to

Author contributions: W.L. and R.W.A. designed research; W.L. performed research; W.L. analyzed data; and W.L. and R.W.A. wrote the paper.

The authors declare no conflict of interest.

[1]To whom corrrespondence should be addressed. E-mail: raldrich@mail.utexas.edu.

This article contains supporting information online at www.pnas.org/lookup/suppl/doi:10.1073/pnas.1103090108/-/DCSupplemental.

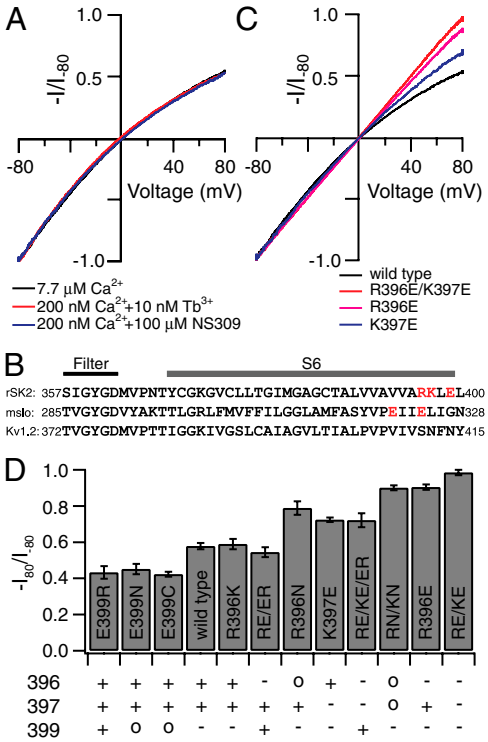

Fig. 1. Charged residues near the inner mouth influence the intrinsic rectification of SK channels. (*A*). Representative SK currents in response to a voltage ramp from −80 mV to 80 mV, recorded under inside-out patch clamp configuration, are normalized to the current level at −80 mV to compare inward rectification. SK currents are activated by 7.7 μM Ca^{2+} (chelated with 5 mM HEDTA) (black), by 10 nM Tb^{3+} added to the Chelex-100 column-treated chelator-free internal solution (contaminating Ca^{2+} approximately 200 nM) (red), or by 200 nM Ca^{2+} (chelated with 5 mM EGTA) in the presence of 100 μM NS309 (blue). (*B*). Alignment of the sequence in the S6 domain between SK (rSK2), BK (mslo), and Kv1.2 K^+ channels. Charged residues of interest in SK and BK channels are highlighted in red. (*C*). Representative SK currents activated by 7.7 μM Ca^{2+} for R396E/K397E (red), R396E (purple), and K397E channels (blue) are normalized and plotted together to compare inward rectification with wild type (black). (*D*). The average levels of inward rectification, characterized by the ratio between current amplitude at 80 mV and that at −80 mV ($-I_{80}/I_{-80}$), were determined from three to six patches for each type of mutant or wild-type channel. Mean value ± SD is plotted for each construct. Expected charges at positions 396, 397, and 399 for wild-type and mutant channels are shown for each construct below the bar graph.

identify the mechanisms for this intrinsic inward rectification, we compared SK channels with large conductance Ca^{2+} activated K^+ (BK) channels. With symmetrical concentration of K^+ ions, K^+ currents through open BK channels demonstrate little rectification. Interestingly, the electrostatic contribution of two negatively charged glutamates (E321, E324) at the end of the S6 transmembrane (TM) domain of BK channels was found to be important for this lack of rectification (10). These negative charges in wild-type BK channels are believed to increase the local concentration of K^+, facilitating outward K^+ conductance and preventing inward rectification. Alignment of SK and BK sequences in the S6 domain indicates that at the positions corresponding to E321 and E324, SK channels have a noncharged valine (V393) and a positively charged arginine (R396), next to another positively charged lysine residue (K397) (Fig. 1*B*). In light of the effect of the negative charges in this region in BK channels, we hypothesized that in SK channels the two positively charged residues R396 and K397 may have the opposite effect, reducing the outward conductance and enhancing inward rectification.

To test this hypothesis, we reversed the charges at R396 and K397 by mutating them into glutamates. As shown in Fig. 1 *C* and *D*, SK currents through double mutant R396E/K397E channels demonstrate little inward rectification ($-I_{80}/I_{-80} = 0.985 \pm 0.015$, mean ± SD, $n = 7$) in contrast to wild type ($-I_{80}/I_{-80} = 0.578 \pm 0.018$, $n = 6$). These results indicate that charge reversal at both R396 and K397 is sufficient to eliminate the observed inward rectification in wild-type channels. To dissect the specific contribution by each of the two residues, we made single mutants R396E and K397E. Inward rectification is mostly eliminated by R396E mutation ($-I_{80}/I_{-80} = 0.904 \pm 0.015$, $n = 8$), but only moderately reduced by K397E mutation ($-I_{80}/I_{-80} = 0.724 \pm 0.012$, $n = 6$, Fig. 1 *C* and *D*), suggesting a stronger contribution by R396 than K397 to the inward rectification in wild-type channels, although both clearly contribute based on the comparison of single mutants with WT and double mutant channels.

If the charges at R396 and K397 affect ion conductance as we hypothesized, the charge reversal mutation should also change the amplitude of single-channel current. We therefore measured the single-channel conductance of wild-type and charge reversal mutant channels. Wild-type SK channels demonstrate reduction of single-channel conductance at positive potentials (Fig. 2*A*), with a level of inward rectification (average $-I_{80}/I_{-80} = 0.59$) comparable with that observed in macroscopic currents (Fig. 1*A*). These data indicate that the rectification observed in macroscopic wild-type SK currents is largely due to a voltage-dependent reduction in outward single-channel conductance, rather than a reduction in open probability (P_o), consistent with an earlier study concluding that gating of SK channels is not voltage dependent (11). This also shows that slow pore blockers such as Ba^{2+} do not contribute to the observed rectification, because Ba^{2+} block would lead to a reduction in apparent P_o rather than single-channel conductance. Compared with wild-type channels, R396E/K397E and R396E channels have significantly increased outward single-channel conductance at positive potentials (Fig. 2 *B*, *C*, and *E*). Inward single-channel conductance at negative potentials is only slightly increased. This voltage-dependent enhancement of single-channel conductance significantly reduces or eliminates inward rectification of the current–voltage (*I–V*) relationship (Fig. 2*F*). By comparison, the K397E mutation has a smaller effect on single-channel conductance and the level of rectification (Fig. 2 *D* and *F*), consistent with its effect in macroscopic currents (Fig. 1*C*). For wild-type and all mutant channels, the degree of rectification in single-channel *I–V* relationship (Fig. 2*F*) agrees reasonably well with macroscopic currents driven by voltage ramps (Fig. 1*C*), suggesting that in all cases, the level of inward rectification is largely determined by single-channel conductance.

To further rule out the possibility that charge reversal at R396 and K397 eliminates inward rectification by removal of intracellular divalent block, we compared the block of SK currents by Ba^{2+} at +60 mV between wild-type and R396E/K397E mutant channels. Fig. 3*A* demonstrates that Ba^{2+} blocks the double mutant channels with an apparent affinity ($IC_{50} = 1.73 \pm 0.12$ μM, Hill coefficient $h = 0.98 \pm 0.06$, $n = 4$) that is comparable to wild-type channels ($IC_{50} = 1.53 \pm 0.03$ μM, $h = 1.02 \pm 0.04$, $n = 4$). Although the R396E/K397E mutation does slightly decrease the apparent affinity for Ba^{2+}, this small difference clearly does not contribute significantly to the large reduction in inward rectification for R396E/K397E channels. The very similar Ba^{2+} affinities were somewhat unexpected, because extra negative charges near the inner mouth introduced by the R396E/K397E mutation should conceivably enhance the Ba^{2+} block by increasing its local concentration. Indeed, the charge reversal mutation dramatically speeds up the kinetics of block. Twenty micromolar Ba^{2+} blocks R396E/K397E channels with a 30 times faster rate than wild type (Fig. 3*B*), suggesting an approximately 30-fold increase in the on rate of Ba^{2+} block. On the other hand, the off rate of Ba^{2+} from the channel must also have been enhanced to a similar degree by the charge reversal, given the very similar Ba^{2+}

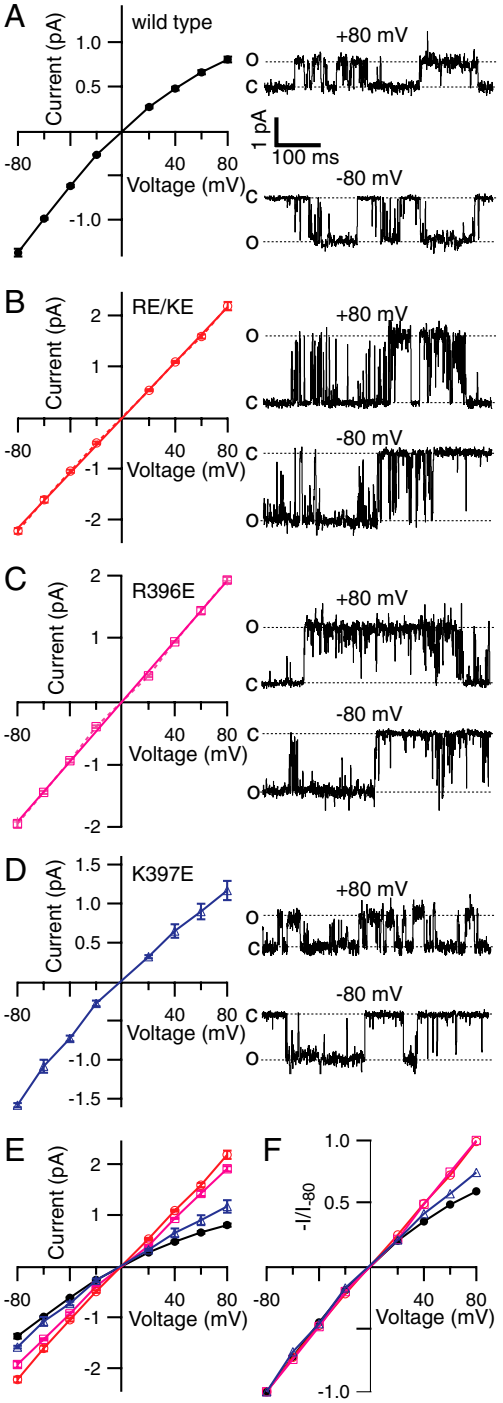

Fig. 2. Inward rectification of SK channels is determined by single-channel conductance. Single-channel current amplitude at different voltages was measured from patches containing one to three channels with multiple-Gaussian fitting of the all-point amplitude histograms. Average amplitudes are plotted as a function of voltage with error bars representing SEM for wild-type (*A*, $n = 5$), R396E/K397E (*B*, $n = 4$), R396E (*C*, $n = 4$), and K397E channels (*D*, $n = 3$) next to representative single-channel traces at −80 and 80 mV (*Right*). In *B* and *C* the dashed lines in the plot simply connect the data points, whereas the solid lines are linear fits of the data, indicating the lack of inward rectification for R396E/K397E and R396E channels. Results from *A* to *D* are plotted together in *E* to compare single-channel current amplitudes. In *F* *I–V* relationships are normalized to the average current amplitude at −80 mV to compare the level of inward rectification.

affinities between wild-type and R396E/K397E mutant channels. These data suggest that positive charges at R396 and K397 in

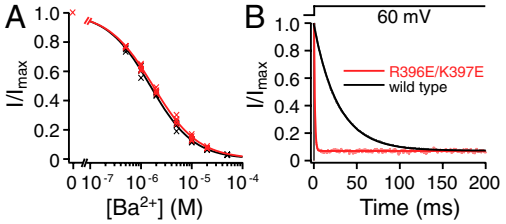

Fig. 3. Comparison of block by Ba^{2+} between wild-type and R396E/K397E channels. (*A*). SK currents were recorded with a 400-ms voltage step to 60 mV from a holding potential of −80 mV. The steady-state current levels with different concentrations of Ba^{2+} were measured at the end of step or determined using single exponential fits of the current traces, then normalized to the control level in the absence of Ba^{2+} and plotted as a function of Ba^{2+} concentration. Data from four patches for wild-type (black crosses) and four patches for R396E/K397E channels (red crosses) were individually fitted with the Hill equation (individual fits not depicted): $I/I_{max} = 1/[1+([Ba^{2+}]/IC_{50})^h]$, where IC_{50} is the half-block Ba^{2+} concentration, and h is the Hill coefficient. Average IC_{50} and h values are reflected by the solid lines for wild-type (black) and R396E/K397E channels (red). (*B*) SK currents were recorded in the presence of 20 μM Ba^{2+} with a voltage step to 60 mV from a holding potential of −80 mV. Currents are normalized to the peak values at the beginning of the voltage step. Current traces are fitted with single exponential time courses (solid lines). Rates of relaxation from the fits in this figure are $1/\tau = 35.2\ s^{-1}$ (wild type, black line), and $1/\tau = 1{,}029.1\ s^{-1}$ (R396E/K397E, red line). Average results from similar experiments are $1/\tau = 35.3 \pm 3.6\ s^{-1}$ (wild type, $n = 4$), and $1/\tau = 1{,}064.8 \pm 69.4\ s^{-1}$ (R396E/K397E, $n = 4$).

wild-type channels constitute an electrostatic energy barrier that slows the flow of Ba^{2+} in both directions, but does not affect the steady-state
equilibrium of the binding site. This finding is consistent with the location of the Ba^{2+} binding site being far away from the inner mouth, near the selectivity filter (6).

To test further whether an electrostatic mechanism accounts for the effects of positive charges on inward rectification, we made other substitutions at these two positions, particularly at R396 due to its stronger effect. Given that in BK channels even neutralization of the endogenous negative charges at this region leads to inward rectification (10), we made charge neutralization mutants at these two positions. R396N/K397N channels ($-I_{80}/I_{-80} = 0.900 \pm 0.014$, $n = 4$, Fig. 1*D* and Fig. S1*A*) also demonstrate much reduced inward rectification compared with wild-type but slightly more than R396E/K397E mutant. R396N channels ($-I_{80}/I_{-80} = 0.789 \pm 0.037$, $n = 4$, Fig. 1*D* and Fig. S1*B*) have less inward rectification than wild-type but more than R396N/K397N mutant, consistent with the smaller but significant effect of the charge at K397. The effect of charge neutralization suggests that positive charges are necessary for the strong inward rectification observed in wild-type channels. On the other hand, R396K mutant channels have very similar levels of inward rectification ($-I_{80}/I_{-80} = 0.589 \pm 0.028$, $n = 5$, Fig. 1*D* and Fig. S1*C*) compared with wild-type channels, indicating that the charge, but not the identity of the residue at this position, is important for rectification.

If a local electrostatic effect is the mechanism, other charged residues near R396 and K397 may also influence the level of inward rectification. We therefore looked at the effect of a nearby glutamate, E399 (Fig. 1*B*). The charge reversal mutant E399R and the neutralization mutant E399N channels can be expressed effectively in Xenopus oocytes. However, they both demonstrate fast and complete rundown of activity even in the presence of saturating Ca^{2+} after the patch was excised. The mechanism for this rundown is unknown to us, but it may suggest that E399 is important for the stability of channel function. Nevertheless, we were able to measure the level of rectification for E399R and E399N channels right after patch excision. Both mutants demonstrate even stronger inward rectification than wild-type channels (E399R: $-I_{80}/I_{-80} = 0.433 \pm 0.035$, $n = 6$, Fig. 1*D* and Fig. S1*D*;

E399N: $-I_{80}/I_{-80} = 0.451 \pm 0.029$, $n = 4$, Fig. 1*D* and Fig. S1*E*). E399C mutant channels demonstrate slower and less rundown of channel activity, but a similar level of inward rectification ($-I_{80}/I_{-80} = 0.423 \pm 0.014$, $n = 5$, Fig. 1*D* and Fig. S1*F*) as the other two E399 mutants. These data indicate that the negative charge at E399 in wild-type channels contributes to reducing the level of inward rectification, counteracting the effect of positive charges at R396 and K397. Indeed, double mutant R396E/E399R channels demonstrate very similar levels of inward rectification ($-I_{80}/I_{-80} = 0.545 \pm 0.027$, $n = 6$, Fig. 1*D* and Fig. S1*G*) as wild-type channels, suggesting that charge effects at 396 and 399 can compensate for each other, consistent with a local electrostatic mechanism. Interestingly, R396E/E399R mutant channel activity does not run down as single mutants at E399, suggesting that the local electrostatic effect, rather than the specific residue identity of E399, may also be the mechanism for regulating the stability of channel function. Rectification in triple mutant R396E/K397E/E399R channels ($-I_{80}/I_{-80} = 0.721 \pm 0.038$, $n = 4$, Fig. 1*D* and Fig. S1*H*) is less than wild-type and R396E/E399R channels but similar as the single mutant K397E, consistent with the effect of an extra negative charge at 397. Fig. 1*D* summarizes the results for wild-type and all mutant channels, illustrating that the level of inward rectification correlates closely with the polarity of charges at positions 396, 397, and 399, especially when considering that charge at 397 has a weaker effect than those at 396 and 399. This clear correlation strongly corroborates our hypothesis that charged residues near the inner mouth of SK channels determine the level of inward rectification through an electrostatic mechanism.

Charged Residues Near the Inner Mouth Regulate Intrinsic P_o of SK Channels. Mutations at R396, K397, and E399 not only modify inward rectification, but also affect the activation of SK channels. Fig. 4*A* shows that wild-type SK channels are activated by Ca^{2+} with EC_{50} of approximately 1 μM ($EC_{50} = 1.03 \pm 0.11$ μM, $h = 3.7 \pm 0.5$, $n = 5$), consistent with our earlier studies (7, 8). Double charge reversal mutant R396E/K397E channels demonstrate an approximately 5-fold increase in the apparent Ca^{2+} affinity for activation ($EC_{50} = 0.21 \pm 0.03$ μM, $h = 2.7 \pm 0.5$, $n = 4$, Fig. 4 *A* and *B*). Single mutant R396E also has a significantly increased apparent Ca^{2+} affinity ($EC_{50} = 0.27 \pm 0.02$ μM, $h = 3.3 \pm 0.3$, $n = 5$, Fig. 4 *A* and *B*). By contrast, the K396E mutation only slightly enhances it ($EC_{50} = 0.83 \pm 0.12$ μM, $h = 4.5 \pm 1.0$, $n = 4$, Fig. 4 *A* and *B*). Comparison of the dose-response relationships in Fig. 4*A* indicates that, as in the case of the rectification, the charge at position 396 has a stronger effect than that at 397 on the apparent Ca^{2+} affinity of activation, although charges at both positions do contribute.

The increased apparent Ca^{2+} affinity by charge reversal mutation could result from several different mechanisms. Ca^{2+} does not bind directly to SK channels, but rather to the constitutively associated calmodulins (3). Therefore it is unlikely that the charges near the inner mouth would contribute directly to the actual Ca^{2+} binding affinity. Estimate of the Debye length under the recording condition (140 mM K^+) yields a value of approximately 8 Å, beyond which electrostatic effect on the local concentration of ions should be minimal. It is therefore also unlikely that these charges significantly affect the effective Ca^{2+} concentration near the binding sites in calmodulin, which are likely to be further removed. Alternatively, the increased apparent Ca^{2+} affinity could result from enhanced coupling between calmodulin and the SK channel, similar to the mechanism proposed for the SK channel enhancer NS309 (8). However, we observed a significant increase in the P_o of channels in the absence of Ca^{2+} (<1 nM) in the charge reversal mutants (Fig. 5), arguing against a mechanism based solely on the coupling of ligand binding to gating. On the other hand, considering allosteric coupling between the channel gate and the Ca^{2+} binding sites, an increase in the constitutive

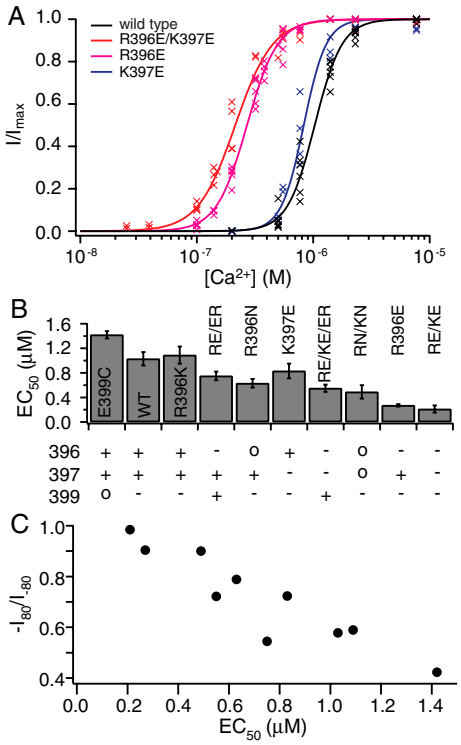

Fig. 4. Charged residues near the inner mouth influence the apparent Ca^{2+} affinity for SK channel activation. (*A*). Mean current levels at −80 mV in the presence of different Ca^{2+} concentrations were measured and normalized to the maximal current level in saturating Ca^{2+} and plotted as a function of Ca^{2+} concentration. Data points from three to six patches for each channel type are plotted together (crosses). Data from each individual patch were fitted with a Hill equation $I/I_{max} = 1/[1 + (EC_{50}/[Ca^{2+}])^h]$, where EC_{50} is the Ca^{2+} concentration at which channels open at the half-maximal level, and h is the Hill coefficient. Average results from individual fits are represented as the solid lines for wild-type (black), R396E/K397E (red), R396E (pink), and K397E channels (blue). (*B*). Average EC_{50} values from the Hill fits are plotted with SD for wild-type and all mutant channels, whereas the charges at positions 396, 397, and 399 for each channel type are shown below the bar graph. *C*). Correlation between the level of inward rectification and EC_{50} for wild type and all mutant channels.

P_o independent of Ca^{2+} could conceivably also increase the apparent Ca^{2+} binding affinity. Although possible contributions by the other mechanisms cannot be completely ruled out, we believe that the majority of the gating effect by charge reversal is likely due to the significant increase in the intrinsic P_o of SK channels in the absence of Ca^{2+}. This conclusion is based on our analyses of the unliganded gating of SK channels. As shown in Fig. 5*A*, wild-type SK channels rarely open in the absence of Ca^{2+}. Indeed the unliganded P_o is so low that it makes difficult accurate measurements. Based on the recordings at single-channel resolution from membrane patches containing large numbers of channels (Fig. 5*A*) our estimate of the unliganded P_o is below 10^{-5}. However, R396E/K397E and R396E channels demonstrate significantly higher P_os in the absence of Ca^{2+} (Fig. 5 *B* and *C*). Single R396E/K397E channels are open 1–2% of the time in the absence of Ca^{2+}, whereas R396E channels are open approximately 0.5% of the time. These observations are consistent with measurements of P_o using macroscopic currents (such as in Fig. 5*D*), by the ratio between the current level in the absence of Ca^{2+} and the maximal level in saturating Ca^{2+} (R396E/K397E: $P_o = 0.020 \pm 0.007$, $n = 8$; R396E: $P_o = 0.006 \pm 0.003$, $n = 8$). These estimates indicate that charge reversal at R396 and K397 increases the unliganded P_o by at least three orders of magnitude. As discussed below, this large increase is sufficient to explain the 4- to 5-fold increase in the apparent Ca^{2+} affinity.

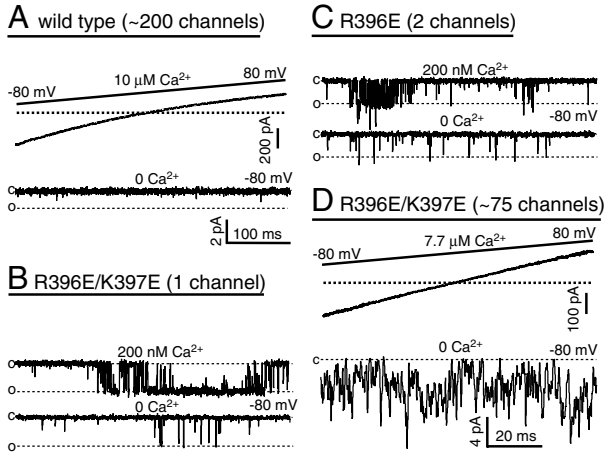

Fig. 5. Charge reversal at R396 and K397 increases the P_o of SK channels in the absence of Ca^{2+}. (*A*). Wild-type SK currents activated with a saturating 10 μM Ca^{2+} in response to a voltage ramp from −80 to 80 mV (*Top*). Based on the amount of total current at −80 mV and the average single-channel current amplitude at −80 mV (Fig. 2*A*), this patch has approximately 200 SK channels. The patch was then treated with nominally Ca^{2+}-free solution (0 Ca^{2+}) and current was recorded at a holding potential of −80 mV (*Bottom*). The dashed line indicates the expected single-channel current level. The scale bar is the same for single-channel records in *A*–*C*. (*B*). Single-channel recording at −80 mV from a membrane patch containing R396E/K397E channels. In the presence of 200 nM Ca^{2+}, the channel opens frequently with no double opening, suggesting a single channel in the patch (*Top*). This channel occasionally opens in 0 Ca^{2+} (*Bottom*). (*C*). Single-channel recording from a patch containing R396E channels at −80 mV in the presence of 200 nM Ca^{2+} (*Top*). Based on the overall P_o and the presence of double opening, two channels are likely to be present in this patch. R396E channels occasionally open in 0 Ca^{2+} (*Bottom*). (*D*). P_o of unliganded R396E/K397E channels was estimated by the ratio between the average current level in 0 Ca^{2+} (*Bottom*) and the average current in 7.7 μM Ca^{2+} at −80 mV (*Top*).

Analyses of the effects of other mutations at R396, K397, and E399 on apparent Ca^{2+} affinity suggest that these charged residues likely regulate channel gating also through an electrostatic mechanism. Charge neutralization mutant R396N/K397N channels have an intermediate apparent Ca^{2+} affinity ($EC_{50} = 0.49 \pm 0.11$ μM, $h = 3.2 \pm 0.6$, $n = 4$, Fig. 4 *B* and Fig. S2*A*) between wild-type and charge reversal mutant channels. R396N channels have slightly lower apparent Ca^{2+} affinity ($EC_{50} = 0.63 \pm 0.11$ μM, $h = 4.9 \pm 0.5$, $n = 3$, Fig. 4*B* and Fig. S2*B*) than R396N/K397N channels, consistent with the effect of the positive charge at K397. R396K channels demonstrate very similar apparent Ca^{2+} affinity ($EC_{50} = 1.09 \pm 0.14$ μM, $h = 4.2 \pm 0.9$, $n = 5$, Fig. 4*B* and Fig. S2*C*) as wild-type channels, suggesting that the charge, but not the identity of residue at 396, is important for gating. Fast and complete rundown of E399R and E399N channel activities precluded reliable measurements of the dose-response relationships. However, E399C channels demonstrate less and slower rundown, allowing us to measure the dose–response relationship with correction for rundown. E399C channels demonstrate reduced apparent Ca^{2+} affinity ($EC_{50} = 1.42 \pm 0.06$ μM, $h = 3.1 \pm 0.3$, $n = 3$, Fig. 4*B* and Fig. S2*D*) compared with wild-type channels, suggesting that the negative charge at E399 in wild-type channels facilitates channel opening, counteracting the effect of the positive charges at R396 and K397. Double mutant R396E/E399R channels have stable activity and slightly enhanced apparent Ca^{2+} affinity ($EC_{50} = 0.75 \pm 0.07$ μM, $h = 3.0 \pm 0.2$, $n = 5$, Fig. 4*B* and Fig. S2*E*) compared with wild-type channels. In contrast to the case of inward rectification where the charges at 396 and 399 seem to perfectly compensate for each other, it seems that charge at 396 has a slightly stronger effect on gating than that at 399. Similarly, the triple mutant R396E/K397E/E399R has a higher apparent Ca^{2+} affinity ($EC_{50} = 0.55 \pm 0.06$ μM, $h = 4.7 \pm 0.6$, $n = 4$, Fig. 4*B* and Fig. S2*F*) than the single mutant K397E. Overall the apparent Ca^{2+} affinity for wild-type and mutant channels correlates closely with the polarity of charges at 396, 397, and 399 (Fig. 4*B*). Positive charges in this region reduce apparent Ca^{2+} affinity, whereas negative charges enhance it. Additionally, except for R396E/E399R and R396E/K397E/E399R mutant channels, there is a clear correlation between the level of inward rectification and the apparent Ca^{2+} affinity (Fig. 4*C*), suggesting that an electrostatic mechanism is involved in both of these two effects.

Discussion

We have investigated the contribution of charged residues near the inner mouth of SK channel pore to single-channel conductance, inward rectification, and gating. Our data suggest that the collective electrostatic effects of these charged residues play important roles in determining both the conductance and the intrinsic gating of the SK channel pore.

Function of ion channels depends on both gating and the open conductance. The inward rectification and small outward conductance of SK channels are physiologically relevant because K^+ efflux normally underlies their functions. The molecular mechanisms for the small conductance and inward rectification are not well understood. Previously, it was shown with both expressed and endogenous SK channels that intracellular divalent ions can block SK channels in a voltage-dependent fashion, resulting in apparent inward rectification (5, 12). These findings have led to the general belief that the inward rectification of SK channels is entirely due to block of outward current by divalent ions such as Ca^{2+} and Mg^{2+}, as in the case for inward rectifier K^+ channels (13). Although block by divalent ions can obviously contribute, we demonstrated in this study that inward rectification is also an intrinsic property of the SK channel pore, independent of intracellular divalent ions. We then established that the intrinsic inward rectification is largely due to a voltage-dependent reduction in outward single-channel conductance.

Previous findings with BK channels (10, 14) suggest a possible electrostatic mechanism for single-channel conductance and inward rectification in SK channels. Alignment between SK and BK channels identifies three charged residues near the end of S6 TM domains lining the pore of SK channels R396, K397, and E399. Charge reversal and neutralization at these three positions have dramatic effects on the single-channel conductance and inward rectification. To help understand the mechanisms for the mutational effects, we constructed a structural model of SK channel (Fig. 6) by threading its sequence in the pore region into the crystal structure of Kv1.2 potassium channel (15) [Protein Data Bank (PDB) ID code 2A79]. Given that the sequence of SK S6 domain is quite different from that of Kv1.2 (approximately 30% identity, Fig. 1*B*) or any other K^+ channels with solved structures, this model is intended only for gross guidelines. The model suggests that the charged residues provide a ring of charges around the inner mouth that control the energy barrier for the entry and the exit of K^+ ions by an electrostatic mechanism (Fig. 6). This hypothesis is supported by our data.

Charge reversal mutations at R396 and K397 abolish the inward rectification by more strongly increasing outward than inward single-channel conductance, consistent with the previous finding in BK channels that negative charges in this region enhance outward conductance and prevent inward rectification (10, 14). The effect of charge reversal at R396 and K397 on single-channel conductance suggests that positively charged residues at these positions in wild-type channels contribute to the small conductance of SK channels. Indeed, R396E/K397E channels have a single-channel conductance of approximately 30 pS, comparable to or higher than most other K^+ channels. However, other factors must also contribute to SK channels' smallest conductance among Ca^{2+} activated K^+ channels, given that intermediate conductance Ca^{2+} activated K^+ (IK) channels have

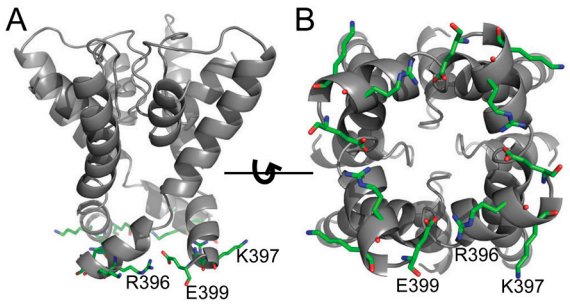

Fig. 6. Structural model of the SK channel pore based on the Kv1.2 structure. Sequence of rSK2 was threaded into the structure of Kv1.2 using the "SwissModel" function in Swiss-PdbViewer software. (*A*). A view of the model from the side of the channel pore. R396, K397, and E399 are shown as sticks. Nitrogen atoms are shown in blue and oxygen atoms in red. (*B*). A view of the model from the intracellular side of the channel pore.

significantly larger single-channel conductance but with conserved sequence with SK channels near the inner mouth including all three charged residues (16). In fact, the negative charges near the inner mouth of BK channels also increase the single-channel conductance only by a factor of 2, incapable of explaining their uniquely large single-channel conductance (10, 14). Instead, other factors such as the diameter of inner pore may contribute significantly to determining the single-channel conductance of K^+ channels (17, 18).

Several findings with mutations at R396, K397, and E399 demonstrate that the level of inward rectification is determined by a local electrostatic mechanism. First, charges at R396, K397, and E399 all affect rectification but with different importance; second, charge neutralizations at R396 and K397 have intermediate effects between wild type and charge reversal; third, charges at positions 396 and 399 can perfectly compensate for each other; finally, with all mutant and wild-type channels considered, there is a clear correlation between the level of rectification and the overall number and polarity of charges at these three positions, such that more positive charges result in stronger inward rectification.

Interestingly, our structural model for SK channels provides straightforward explanations for several of the observed mutational effects. The localization of these charged residues surrounding the inner mouth suggests that they collectively contribute to the energy barrier for entry of K^+ ions. Therefore positive charges at these positions hinder K^+ entry, whereas negative charges facilitate it. Additionally, the model posits the side chains of R396 and E397 near the central pore, whereas the side chain of K397 points away, consistent with our observation that the charge at K397 has a smaller effect on rectification than those at R396 and E399. Finally, the model places the charged moiety of R396 near that of E399 from a neighboring subunit, which can easily explain why the charges at these two positions compensate for each other in controlling inward rectification (Fig. 6). Given the large difference in sequence between the S6 domains of SK and Kv1.2 channels, it would not be surprising if our structural model deviates significantly from the actual SK pore structure in terms of the orientation and pore exposure of side chains. However, our findings suggest that the structural model likely predicts correctly the position and orientation of these charged residues.

The effect of charge reversal at R396 and K397 on the Ba^{2+} block is also consistent with an electrostatic mechanism. The R396E/K397E mutation increases both the on rate and the off rate of Ba^{2+} by approximately 30-fold. The charges at positions 396 and 397 likely contribute to the height of the energy barrier near the inner mouth and control the rate of Ba^{2+} entering or leaving the inner pore, but do not affect the binding affinity of Ba^{2+} in equilibrium because they are far away from the Ba^{2+} binding site (6). In a nonequilibrium process such as conduction of K^+ through the pore, this energy barrier will have a direct impact on the rate of conductance if it is a rate-limiting step. Charge reversals at R396 and K397 also increase the inward single-channel conductance, albeit slightly (Fig. 2). Therefore this energy barrier likely also affects the exit rate of K^+ from the pore, although it seems to be more rate-limiting for outward than for inward conductance. Here we interpret our data using an energy barrier limiting the rates for cations going in both directions, rather than changes in effective local concentrations due to a "surface charge effect" (19, 20), which cannot easily explain the increased inward conductance and Ba^{2+} off rate.

The electrostatic effect of charged residues near the channel entrance is also employed to control conductance and rectification by other cation channels such as acetylcholine receptor channels (21) and ryanodine receptor channels (22), and anion channels such as cystic fibrosis transmembrane conductance regulator chloride channels (20) and glycine receptor channels (23). In most of these cases, residues carrying the opposite charge of the permeating ions surround the inner or outer mouth of the pore and enhance conductance. In contrast, in SK channels positive charges near the inner mouth function to reduce conductance and result in inward rectification.

Our results show that mutations at the charged residues R396, K397, and E399 also affect the apparent Ca^{2+} affinity for SK channel activation and the intrinsic P_o of unliganded channels, suggesting the involvement of these residues in the gating energetics. Unliganded wild-type SK channels are very tightly closed and rarely open spontaneously ($P_o < 10^{-5}$), indicating that the closed state of the channel is strongly favored relative to the open state in the absence of Ca^{2+}, and a large amount of energy is required from the binding of Ca^{2+} at calmodulin to drive the channel open. The mechanism for this tight closure is currently unknown. However, our finding that charge reversal at R396 and K397 increases the unliganded P_o by over three orders of magnitude suggests that the positive charges at these residues contribute significantly to stabilizing the closed state relative to the open state in wild-type SK channels.

Considering the allosteric coupling between channel gating and Ca^{2+} binding at calmodulin, the large increase in the intrinsic equilibrium constant (L_0) for the Closed ↔ Open transition by charge reversal at R396 and K397 should also increase the apparent Ca^{2+} affinity for activation. So can the thousandfold increase in the intrinsic L_0 explain the observed approximately 5-fold decrease in EC_{50} for R396E/K397E channels? The Hill equation is a completely empirical description of the dose–response relationship that unfortunately has no physical foundations to account for an allosteric model of gating. As a result, the effect of increase in L_0 on the apparent EC_{50} is not defined in the Hill equation itself. The exact relationship between parameters of empirical Hill fits and the nature of an allosteric gating model is rather complicated and beyond the scope of this paper (24), and an allosteric gating model for SK channels has not been established. However, rough comparison between any allosteric model and the Hill equation suggests that the change in intrinsic L_0 is sufficient to explain the change in apparent Ca^{2+} affinity. As an approximation, we discuss the case using $h = 4$, an average value from the fittings. Comparing the Hill fit $P_o = 1/(1+(EC_{50}/[Ca^{2+}])^4)$ with $P_o = L/(1+L)$ (L is the equilibrium constant for the Closed ↔ Open transition), if a mechanism can enhance Ca^{2+} binding such that the EC_{50} is decreased by 5-fold, it would increase L by 5^4, or 625-fold at a given Ca^{2+} concentration. Now if we consider an allosteric mechanism that predicts that enhancement of the Closed ↔ Open transition should conversely increase the apparent Ca^{2+} affinity, the R396E/K397E mutation, which enhances intrinsic L_0, and proportionally L (L is linearly dependent on L_0 with an allosteric model), by a thousandfold independently of Ca^{2+}, should enhance Ca^{2+} binding

such that the EC_{50} is decreased by $1{,}000^{1/4}$, or 5- to 6-fold, as we have observed experimentally. This analysis is independent of the exact allosteric gating model of SK channels, as long as the model remains the same for wild-type and charge reversal mutants, and the data in both cases can be well fitted by the Hill equation with $h = 4$. As an example in a previous study that thoroughly discussed the Hill fits of allosteric models (24), when the behavior of an allosteric model under special conditions can be sufficiently fitted with the Hill equation with $h = 4$, a thousandfold increase in the Closed ↔ Open equilibrium constant indeed leads to 5- to 6-fold decrease in EC_{50}, consistent with our analysis above. Comparison between R396E/K397E and R396E mutants lends further support to our analysis. The P_o for unliganded R396E/K397E channels (approximately 0.02) is about 3-fold of that for R396E channels (approximately 0.006). Our analysis predicts that the EC_{50} for R396E channels should be about $3^{1/4}$, or 1.3-fold of that for R396E/K397E channels, which was exactly the difference between the EC_{50}s we observed (0.27 μM and 0.21 μM, respectively). Other mutants that we made have significantly lower unliganded P_os, precluding accurate estimates and this type of analysis. Altogether our data and analyses suggest that the gating effect of the charged residues near the inner mouth is largely through controlling the intrinsic gating transition of channels independent of Ca^{2+}.

Comparison of the gating between wild-type and all mutant channels at R396, K397, and E399 suggests that in wild-type SK channels positive charges near the inner mouth stabilize the closed state of the channel relative to the open state, whereas negative charges have the opposite effect. The actual mechanism for this effect is unclear, although both the dependence of EC_{50} on overall charges and its clear correlation with level of rectification suggest that the mechanism is likely also electrostatic in nature. However, it remains to be revealed how the intrinsic gating energetics of SK channels is influenced by an electrostatic mechanism near the inner mouth. One interesting possibility is that the charges in this region may affect the occupancy of a nearby K^+ binding site, and the occupancy of this site may be important for gating energetics. Therefore positive charges can reduce the occupancy of this site through an electrostatic repulsion and stabilize the closed state relative to the open state, whereas negative charges have the opposite effect. Indeed, it has been widely accepted that K^+ occupancy can significantly affect the gating of K^+ channels (25–27). Particularly, a previous study on Shaker K^+ channels discovered that the occupancy of a K^+ binding site near the inner mouth can indirectly affect the C-type inactivation gate near the selectivity filter (28, 29), which is the gate location proposed for SK channels (30, 31). Additionally, in the present study, charge reversal or neutralization at E399 causes the channels to run down, also reminiscent of a so-called "defunct state" of K^+ channels resulting from reduction in K^+ occupancy (32). As an alternative to the occupancy hypothesis, the cluster of charges near the inner mouth may interact with other charged parts of the channel complex, contributing to gating energetics with an electrostatic mechanism. Because positively and negatively charged residues have opposite effects compared with neural residues, the degree of exposure by these charged residues to a polar environment likely does not contribute significantly to the observed changes in gating energetics.

Materials and Methods

Channel Expression and Molecular Biology. Wild-type and mutant rSK2 (KCa2.2) channels were expressed in Xenopus oocytes by injection of corresponding RNAs transcribed in vitro. Approximately 10 ng RNA was injected into each oocyte for macroscopic recordings and approximately 0.1–0.5 ng for single-channel recordings. Wild-type rSK2 DNA was a kind gift from the Adelman lab (Vollum Institute, Portland, OR), whereas the mutants were generated in the lab using the Quickchange mutagenesis kit (Stratagene). All constructs were subcloned into or generated in the pOX vector and verified by sequencing.

Electrophysiology. Inside-out patch clamp recordings were typically performed on oocytes 4–10 d after injection. All experiments were conducted at approximately 22 °C. Electrodes for macroscopic recordings were made from borosilicate glass pipets (VWR Scientific, Cat. No. 53432-921), whereas those for single-channel recordings were made from 8250-type glass pipets (A-M Systems, Inc., Cat. No. 593200). Electrodes were coated with Sticky Wax (Kerr Corporation) and fire-polished before use. Data were recorded using an Axopatch 200A Amplifier (Molecular Devices, Inc.) coupled with an ITC-16 interface (HEKA Electronik). Data were filtered at 5 KHz using the built-in filter of the amplifier and sampled at 50 KHz (macroscopic current) or 100 KHz (single-channel current) using the *Pulse* acquisition software (HEKA Electronik). Single-channel current records were digitally filtered at 1 or 2 KHz before analysis using QUB software. Single-channel current amplitudes at different voltages were determined by multiple-Gaussian fitting of the all-point amplitude histograms constructed from the data after baseline correction. In measurements of the dose–response relationships for Ca^{2+}-dependent activation and Ba^{2+}-dependent block, occasional experiments with severe channel rundown (>15%) were excluded from analysis, whereas those with small rundown were corrected using a linear extrapolation for the time course of rundown.

Internal base solution (IBS) contained (in mM): 136 $KMeSO_3$, 20 Hepes, 6 KCl, pH = 7.2. Extracellular (pipette) solution was prepared by adding 2 mM $MgCl_2$ to the IBS. Internal (bath) solutions containing various amounts of free Ca^{2+} were prepared by adding 5 mM Ca^{2+} chelators (EGTA for $[Ca^{2+}] < 0.5$ μM, hydroxyethyl ethylenediamine triacetic acid (HEDTA) for $[Ca^{2+}] \geq 0.5$ μM) and an appropriate amount of $CaCl_2$ to the IBS. The final free Ca^{2+} concentrations in the internal solutions were either directly measured with a Ca^{2+} electrode (Orion Research, Inc.) or calculated using experimentally determined affinities for EGTA and HEDTA in the same IBS with the Ca^{2+} electrode. Solutions with 5 mM EGTA and no added Ca^{2+} were considered nominally Ca^{2+} free (estimated to be <1 nM). Current traces in the presence of this nominally Ca^{2+}-free solution were often used to estimate and subtract leak current for analysis. In cases where channels were not fully closed in Ca^{2+}-free solution and single-channel openings became recognizable, the minimal current level in the current trace was instead used for leak subtraction. Given that the P_o in these cases is less than 2%, such leak subtraction has only a marginal effect on the dose–response relationships or levels of inward rectification. Solution changes were achieved by washing with new solution of >10 times the chamber volume. In experiments using Tb^{3+} to activate SK channels, internal solutions were prepared by passing the IBS through a column made from Chelex-100 resin to remove contaminating divalent ions. $TbCl_3$ was then added to achieve the desired Tb^{3+} concentrations. In experiments measuring blockage of SK current by Ba^{2+}, 10 μM $CaCl_2$ and varying amounts of $BaCl_2$ were added to the column-treated chelator-free IBS to prepare solutions that saturate the activation of SK channels but with different concentrations of Ba^{2+}. All chemicals were obtained from Sigma-Aldrich.

ACKNOWLEDGMENTS. The authors thank Dr. Adron Harris (University of Texas, Austin, TX) for providing Xenopus oocytes, and Dr. John Adelman (Vollum Institute, Portland, OR) for the rSK2 construct used in this study.

1. Pedarzani P, Stocker M (2008) Molecular and cellular basis of small- and intermediate-conductance, calcium-activated potassium channel function in the brain. *Cell Mol Life Sci* 65:3196–3217.
2. Faber ES (2009) Functions and modulation of neuronal SK channels. *Cell Biochem Biophys* 55:127–139.
3. Xia XM, et al. (1998) Mechanism of calcium gating in small-conductance calcium-activated potassium channels. *Nature* 395:503–507.
4. Maylie J, Bond CT, Herson PS, Lee WS, Adelman JP (2004) Small conductance Ca^{2+}-activated K^+ channels and calmodulin. *J Physiol* 554:255–261.
5. Soh H, Park CS (2001) Inwardly rectifying current-voltage relationship of small-conductance Ca^{2+}-activated K^+ channels rendered by intracellular divalent cation blockade. *Biophys J* 80:2207–2215.
6. Soh H, Park CS (2002) Localization of divalent cation-binding site in the pore of a small conductance Ca(2+)-activated K(+) channel and its role in determining current-voltage relationship. *Biophys J* 83:2528–2538.
7. Li W, Aldrich RW (2009) Activation of the SK potassium channel-calmodulin complex by nanomolar concentrations of terbium. *Proc Natl Acad Sci USA* 106:1075–1080.
8. Li W, Halling DB, Hall AW, Aldrich RW (2009) EF hands at the N-lobe of calmodulin are required for both SK channel gating and stable SK-calmodulin interaction. *J Gen Physiol* 134:281–293.

9. Strobaek D, et al. (2004) Activation of human IK and SK Ca^{2+}-activated K^+ channels by NS309 (6,7-dichloro-1H-indole-2,3-dione 3-oxime). *Biochim Biophys Acta* 1665:1–5.
10. Brelidze TI, Niu X, Magleby KL (2003) A ring of eight conserved negatively charged amino acids doubles the conductance of BK channels and prevents inward rectification. *Proc Natl Acad Sci USA* 100:9017–9022.
11. Hirschberg B, Maylie J, Adelman JP, Marrion NV (1998) Gating of recombinant small-conductance Ca-activated K^+ channels by calcium. *J Gen Physiol* 111:565–581.
12. Ledoux J, Bonev AD, Nelson MT (2008) Ca^{2+}-activated K^+ channels in murine endothelial cells: Block by intracellular calcium and magnesium. *J Gen Physiol* 131:125–135.
13. Lu Z (2004) Mechanism of rectification in inward-rectifier K^+ channels. *Annu Rev Physiol* 66:103–129.
14. Nimigean CM, Chappie JS, Miller C (2003) Electrostatic tuning of ion conductance in potassium channels. *Biochemistry* 42:9263–9268.
15. Long SB, Campbell EB, Mackinnon R (2005) Crystal structure of a mammalian voltage-dependent Shaker family K^+ channel. *Science* 309:897–903.
16. Ishii TM, et al. (1997) A human intermediate conductance calcium-activated potassium channel. *Proc Natl Acad Sci USA* 94:11651–11656.
17. Li W, Aldrich RW (2004) Unique inner pore properties of BK channels revealed by quaternary ammonium block. *J Gen Physiol* 124:43–57.
18. Brelidze TI, Magleby KL (2005) Probing the geometry of the inner vestibule of BK channels with sugars. *J Gen Physiol* 126:105–121.
19. Green WN, Andersen OS (1991) Surface charges and ion channel function. *Annu Rev Physiol* 53:341–359.
20. Aubin CN, Linsdell P (2006) Positive charges at the intracellular mouth of the pore regulate anion conduction in the CFTR chloride channel. *J Gen Physiol* 128:535–545.
21. Imoto K, et al. (1988) Rings of negatively charged amino acids determine the acetylcholine receptor channel conductance. *Nature* 335:645–648.
22. Xu L, Wang Y, Gillespie D, Meissner G (2006) Two rings of negative charges in the cytosolic vestibule of type-1 ryanodine receptor modulate ion fluxes. *Biophys J* 90:443–453.
23. Moorhouse AJ, Keramidas A, Zaykin A, Schofield PR, Barry PH (2002) Single channel analysis of conductance and rectification in cation-selective, mutant glycine receptor channels. *J Gen Physiol* 119:411–425.
24. Weiss JN (1997) The Hill equation revisited: Uses and misuses. *FASEB J* 11:835–841.
25. Baukrowitz T, Yellen G (1995) Modulation of K^+ current by frequency and external [K+]: A tale of two inactivation mechanisms. *Neuron* 15:951–960.
26. Piskorowski RA, Aldrich RW (2006) Relationship between pore occupancy and gating in BK potassium channels. *J Gen Physiol* 127:557–576.
27. Lopez-Barneo J, Hoshi T, Heinemann SH, Aldrich RW (1993) Effects of external cations and mutations in the pore region on C-type inactivation of Shaker potassium channels. *Receptor Channel* 1:61–71.
28. Ogielska EM, Aldrich RW (1999) Functional consequences of a decreased potassium affinity in a potassium channel pore. Ion interactions and C-type inactivation. *J Gen Physiol* 113:347–358.
29. Ogielska EM, Aldrich RW (1998) A mutation in S6 of Shaker potassium channels decreases the K^+ affinity of an ion binding site revealing ion-ion interactions in the pore. *J Gen Physiol* 112:243–257.
30. Bruening-Wright A, Schumacher MA, Adelman JP, Maylie J (2002) Localization of the activation gate for small conductance Ca^{2+}-activated K^+ channels. *J Neurosci* 22:6499–6506.
31. Bruening-Wright A, Lee WS, Adelman JP, Maylie J (2007) Evidence for a deep pore activation gate in small conductance Ca^{2+}-activated K^+ channels. *J Gen Physiol* 130:601–610.
32. Gomez-Lagunas F (1997) Shaker B K^+ conductance in Na^+ solutions lacking K^+ ions: A remarkably stable non-conducting state produced by membrane depolarizations. *J Physiol* 499(Pt 1):3–15.